Medicinal Chemistry Research (2019) 28:984–991
https://doi.org/10.1007/s00044-019-02351-3

MEDICINAL CHEMISTRY RESEARCH

ORIGINAL RESEARCH

Synthesis and cytotoxic effects on pancreatic cancer cells of resveratrol analogs

Barbara De Filippis[1] · Laura De Lellis[2,3] · Rosalba Florio[2,3] · Alessandra Ammazzalorso[1] · Pasquale Amoia[1] · Marialuigia Fantacuzzi[1] · Letizia Giampietro[1] · Cristina Maccallini[1] · Rosa Amoroso[1] · Serena Veschi[2,3] · Alessandro Cama[2,3]

Received: 13 February 2019 / Accepted: 22 April 2019 / Published online: 29 April 2019

Abstract

In this study, a series of resveratrol analogs was synthesized and the effects on the viability of pancreatic cancer cell lines were evaluated. The new molecules were designed by removing the 3- and 5-OH groups of resveratrol, and by incorporating other substituents in 4-position, or by replacing the dihydroxybenzene with other aromatic systems. In all compounds the 4′-OH was kept unaltered. The effects of the compounds on cell viability were analyzed in three pancreatic cancer cell lines with distinct genetic profiles. Several compounds (e.g., **5**, **9**, and **12**) exhibited improved cytotoxic activities as compared to the reference compounds, making them potential candidates for further evaluation as anticancer drugs.

Keywords Antiproliferative · Resveratrol · 4-Hydroxystilbene · Cytotoxicity · Pancreatic cancer

Abbreviations

RSV	resveratrol
PC	pancreatic cancer
SLB	stilbene
4-HSLB	4′-hydroxystilbene
TBSCl	*t*-butyldimethylsilyl chloride
NEt_3	triethylamine
TBAF	*tetra-n*-butylammonium fluoride

Introduction

Resveratrol (*trans*-3,5,4′-trihydroxystilbene, RSV), a well-known natural polyphenolic phytoalexin present in grape skin and red wine, is a component of Asian traditional medicine used to treat cardiovascular diseases. Several studies showed that RSV, as well as its analogs and derivatives, exhibits antioxidant (Sadeghi et al. 2017), anti-inflammatory (de Sá Coutinho et al. 2018), and protective activities against cardiac (Bonnefont-Rousselot 2016), neurodegenerative (Ono et al. 2003; Zhang et al. 2005), and metabolic disorders (Chou et al. 2018; Diaz-Gerevini et al. 2016). RSV has also been reported to have a cancer chemoprotective effect (Huang and Zhu 2011; Elshaer et al. 2018). Since 1997, RSV has also gained considerable attention as anticancer agent (Block et al. 1992; Jang et al. 1997), because of its potential use in chemoprevention and chemotherapy of various tumors, including colon, breast, and prostate cancers, mediated via effects on cell growth, apoptosis, angiogenesis, and metastasis (Carter et al. 2014). The cancer chemoprevention effects of RSV could be mainly attributed to its antioxidant activity (De la Castra and Villegas 2007; Kruk and Aboul-Enein 2017), since free-radical-mediated peroxidation of membrane lipids and oxidative damage of DNA play an important role in cancer (Telek et al. 2001; Shang et al. 2009). The antioxidant mechanism of RSV has been studied in detail and several studies have shown that the OH in 4′-position is essential for the scavenging of free radicals (Queiroz et al. 2009; Garcia et al. 2013; Scherzberg et al. 2015; Deck et al. 2017). The 4′-OH is also responsible for other biological activities; indeed, the interaction between the 4′-hydroxystyryl moiety

These authors contributed equally: Barbara De Filippis, Laura De Lellis

✉ Rosa Amoroso
rosa.amoroso@unich.it

[1] Unit of Medicinal Chemistry, Department of Pharmacy, University of Chieti "G. d'Annunzio", Chieti, Italy

[2] Unit of General Pathology, Department of Pharmacy, University of Chieti "G. d'Annunzio", Chieti, Italy

[3] Center on Aging Sciences and Translational Medicine (Ce.S.I.-MeT), University of Chieti "G. d'Annunzio", Chieti, Italy

and DNA polymerase has been described as a mechanism underlying the inhibition of cell cycle progression (Britton et al. 2015), and 4′-OH in *trans*-configuration was required for inhibition of cell proliferation (Stivala et al. 2001). Pancreatic cancer (PC) is the fourth common cause of cancer death in occidental countries with a very limited median survival time (<6 months) and a 5-year survival time ranging from 1% to 4% (Teague et al. 2015). Surgical resection is the best therapeutic option for PC, but it is possible for less than 20% of patients, since this tumor develops without early symptoms and is frequently diagnosed at advanced stages. At present, systematic chemotherapy includes gemcitabine, the combination of gemcitabine and nab-paclitaxel or, alternately, the Folfirinox protocol (5-FU, leucovorin, irinotecan, and oxaliplatin), although survival outcomes for PC patients remain very poor (Ansari et al. 2016). Moreover, these agents have a significant toxicity that becomes more marked when they are used in combination. Thus, the limited success of current standard therapies underlines an urgent need to identify new therapeutic strategies and agents to treat this deadly disease. In this light, several natural and synthetic molecules, including RSV and its derivatives, have been explored as single agents or in combination with standard chemotherapy in cell and animal models of PC manifesting significant cytotoxicity, thus suggesting their potential as agents for PC prevention and treatment (Ding and Adrian 2002; Xu et al. 2015; Duan et al. 2016; Murty et al. 2016; Tsang et al. 2016; Ammazzalorso et al. 2017; Herrera-R et al. 2018).

Recently, we modified the structure of RSV by introducing various substituents on the two aromatic rings or replacing the distal phenyl with other aromatic rings, and generating hybrids with alkanoic chains, with the aim to act on nuclear receptor PPAR (De Filippis et al. 2011, 2015a, 2015b; Leporini et al. 2017; Giampietro et al. 2012, 2014, 2019; dos Santos et al. 2015) In order to better explore the importance of the stilbene (SLB) scaffold contained in RSV, and taking into account the well-established multiple activities of SLB-containing compounds (De Filippis et al. 2017, 2019; Giacomini et al. 2016; Chillemi et al. 2007; Kondratyuk et al. 2011), in this study we focused on the possibility of changing the structure of RSV to obtain analogs active on PC. Bearing in mind that the 4′-OH was considered essential for the antioxidant/antitumor activity, we synthesized analogs of the RSV in which the 4′-OH was preserved, and the 3,5-OH moiety was replaced with 4-substituted phenols (compounds **1–9**). Other analogs were synthesized by introducing another aromatic ring instead of 3,5-OH phenyl (compounds **10–12**). All new derivatives can be considered analogs of the RSV but also of the 4-hydroxystilbene (4-HSLB, Fig. 1), which was therefore considered in the biological tests as a further reference compound.

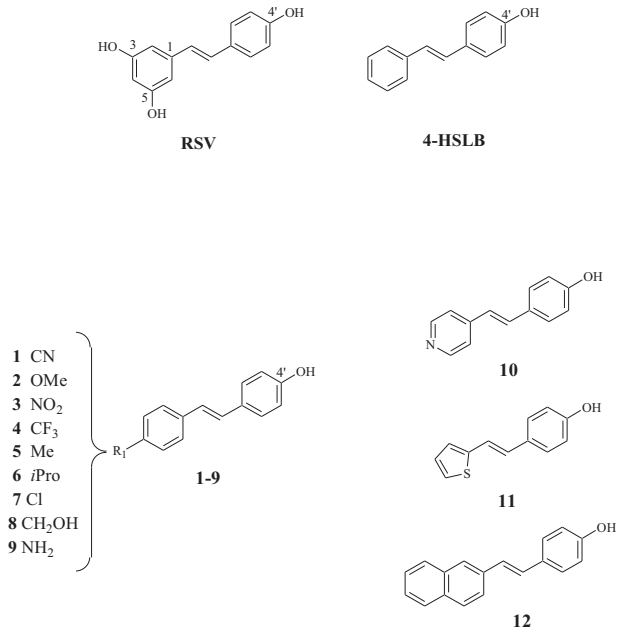

Fig. 1 Resveratrol, 4-hydroxystilbene, and general structure of new analogs **1–12**

We evaluated the cytotoxicity of compounds **1–12** in three PC cell lines, AsPC-1, Capan-2, and BxPC-3, with the aim to identify the influences of substituents added in *p*-position and different aromatics instead of distal phenyl of RSV on the viability of the PC cells.

Materials and methods

Chemistry

General

Commercial reagents, RSV, and 4-HSLB were used as received from Aldrich or Fluka. Flash chromatography was performed on silica gel 60 (Merck) and TLC on F254 silica gel 60 TLC plates. Melting points (m.p.) were determined on a Büchi B-540 apparatus and are uncorrected. Infrared spectra were recorded on an FT-IR 1600 PerkinElmer spectrometer. NMR spectra were run at 300 MHz on a Varian instrument using TMS as internal standard; chemical shifts (δ) are reported in ppm. Microanalyses were carried out with a Eurovector EuroEA3000 model analyzer. Analyses indicated by the symbols of the elements were within ±0.4% of the theoretical values.

Preparation of arylethenylphenols 1–8 and 10–12

A stirred mixture of piperidine (10.23 mmol), appropriately 4-substituted arylacetic acid (4.91 mmol), and 4-hydroxybenzaldeyde (4.09 mmol) was heated gradually to

130 °C. After 4–24 h, the residue was cooled at room temperature (r.t.) and portioned between EtOAc (3 × 30 mL) and water (20 mL). The organic phases were dried over Na_2SO_4 and concentrated under reduced pressure to yield the crude products that were purified by column chromatography (eluent CH_2Cl_2/MeOH 95:5 or cyclohexane/EtOAc 6:4) giving the pure phenols **1–8** and **10–12**.

4-[(*E*)-2-(4-hydroxyphenyl)ethenyl]benzonitrile (1): green solid, 24% yield, m.p. 218–220 °C. ^{1}H NMR (acetone-*d6*) δ 6.87 (d, $J = 8.7$ Hz, 2H), 7.1 (q, $J = 49.5$ Hz, 2H), 7.38 (d, $J = 9.0$ Hz, 2H), 7.51 (q, $J = 12.9$ Hz, 4H); ^{13}C NMR (acetone-*d6*) δ 114.0 ($C_{Ar}CN$), 115.02 (CH_{Ar}), 119.41 (CN), 126.76 (CH_{Ar}), 128.48 (CH_{Ar}), 129.15 (CH=CH), 129.69 (CH=CH), 130.37 (CH_{Ar}), 132.69 (CH_{Ar}), 142.47 (CH_{Ar}), 159.74 (CH_{Ar}), 179.0 (CO); IR (neat) 3313, 2234, 1595, and 1209 cm^{-1}; anal. calc. for $C_{15}H_{11}NO$: C, 81.43; H, 5.01; N, 6.33; O, 7.23; found: C, 81.15; H, 5.00; N, 6.34.

4-[(*E*)-2-(4-methoxyphenyl)ethenyl]phenol (2): yellow solid, 17% yield, m.p. 206–207 °C. ^{1}H NMR (acetone-*d6*) δ 3.79 (s, 3H), 6.83 (d, $J = 8.7$ Hz, 2H), 6.91 (d, $J = 9.0$ Hz, 2H), 7.00 (s, 2H), 7.41 (d, $J = 8.7$ Hz), 7.48 (d, $J = 8.7$ Hz, 2H), 8.44 (s, 1H, OH); ^{13}C NMR (acetone-*d6*) δ 54.88 (CH_3), 114.23 (C_{Ar}), 115.72 (C_{Ar}), 125.47 (CH=CH), 126.48 (CH=CH), 127.52 (C_{Ar}), 127.75 (C_{Ar}), 129.7 (C_{Ar}), 130.8 (C_{Ar}), 157.2 (C_{Ar}), 159.3 ($C_{Ar}OCH_3$); IR (neat) 3423, 3019, 2955, 2838, 2360, 1607, 1514, and 1250 cm^{-1}; anal. calc. for $C_{15}H_{14}O_2$: C, 79.62; H, 6.24; O, 14.14; found: C, 79.35; H, 6.25.

4-[(*E*)-2-(4-nitrophenyl)ethenyl]phenol (3): red solid, 30% yield, m.p. 201 °C dec. ^{1}H NMR (acetone-*d6*) δ 6.89 (d, $J = 8.7$ Hz, 2H), 7.19 (d, $J = 16.5$ Hz, 1H), 7.44 (d, $J = 16.5$ Hz, 1H), 7.54 (d, $J = 8.7$ Hz), 7.79 (d, $J = 8.7$ Hz, 2H), 8.20 (d, $J = 9.0$ Hz, 2H); ^{13}C NMR (acetone-*d6*) δ 115.96 (CH_{Ar}), 123.49 (CH=CH), 124.14 (CH_{Ar}), 126.87 (CH_{Ar}), 128.45 (C_{Ar}), 128.97 (CH_{Ar}), 133.59 (CH=CH), 145.13 (C_{Ar}), 163.26 (C_{Ar}), 190.40 ($C_{Ar}NO_2$); IR (KBr) 3422 (broad), 1585, 1504, 1336, and 1108 cm^{-1}; anal. calc. for $C_{14}H_{11}NO_3$: C, 69.70; H, 4.60; N, 5.81; O, 19.90; found: C, 69.87; H, 4.60; N, 5.80.

4-[(*E*)-2-(4-trifluoromethylphenyl)ethenyl]phenol (4): white solid, 23% yield, m.p. 161–163 °C. ^{1}H NMR (acetone-*d6*) δ 6.87 (d, $J = 8.4$ Hz, 2H, CH_{Ar}), 7.13 (d, $J = 16.2$ Hz, 1H, CH=CH), 7.34 (d, $J = 16.5$ Hz, 1H, CH=CH), 7.50 (d, $J = 8.1$ Hz, 2H, CH_{Ar}), 7.66 (d, $J = 8.4$ Hz, 2H, CH_{Ar}), 7.75 (d, $J = 7.8$ Hz, 2H, CH_{Ar}); ^{13}C NMR (acetone-*d6*) δ 115.85 (CH_{Ar}), 124.08 (CH=CH), 125.65 (q, CH_{Ar}), 126.69 (CH_{Ar}), 128.00 (CH_{Ar}), 128.70 (C_{Ar}), 131.62 (CF_3), 128.70 (CH=CH), 142.27 (C_{Ar}), 158.13 (C_{Ar}); IR (neat) 3614, 3419, 3271, 1599, 1511, 1327, 1254, 1181, and 836 cm^{-1}; anal. calc. for $C_{15}H_{11}F_3O$: C, 68.18; H, 4.20; F, 21.57; O, 6.05; found: C, 68.35; H, 4.22.

4-[(*E*)-2-(4-methylphenyl)ethenyl]phenol (5): white amorphous solid, 21% yield. ^{1}H NMR (acetone-*d6*) δ 2.3 (3H, s), 6.91 (2H, d, $J = 8.7$ Hz), 7.05 (2H, q, $J = 10.8$ Hz), 7.15 (2H, d, $J = 7.8$ Hz), 7.35 (2H, d, $J = 8.4$ Hz), 7.42 (2H, d, $J = 7.2$ Hz); ^{13}C NMR ($CDCl_3$) δ 25.99 (CH_3), 116.09 ($CH_{Ar}C$), 126.22 (CH_{Ar}), 126.88 (CH=CH), 126.95 (CH_{Ar}), 127.72 (CH=CH), 128.77 (CH_{Ar}), 129.45 (CH_{Ar}), 135.46 (CH_{Ar}), 136.75(CH_{Ar}), 158.38 (CH_{Ar}); IR (neat) 3436, 2932, 2853, 1603, 1497.3, and 1263 cm^{-1}; anal. calc. for $C_{15}H_{14}O$: C, 85.68; H, 6.71; Cl, 7.61; O, 6.94; found: C, 85.38; H, 6.72.

4-[(*E*)-2-(4-isopropylphenyl)ethenyl]phenol (6): white solid, 19% yield, m.p. 159−161 °C. ^{1}H NMR (CD_3OD) δ 1.23 (d, $J = 6.6$ Hz, 6H), 2.84–2.92 (m, 1H), 6.76 (d, $J = 8.4$ Hz, 2H), 6.96 (q, $J = 14.4$ Hz, 2H), 7.16 (d, $J = 7.5$ Hz, 2H), 7.37 (d, $J = 2.1$ Hz, 4H); ^{13}C NMR (CD_3OD) δ 23.21 (CH_3), 33.95 (CH), 115.29 (CH_{Ar}), 125.52 (CH=CH), 126.00 (CH_{Ar}), 126.42 (CH_{Ar}), 127.47 (CH=CH), 127.52 (CH_{Ar}), 129.44 (C_{Ar}), 135.73 (C_{Ar}), 147.82 (C_{Ar}), 157.08 ($C_{Ar}OH$); IR (neat) 3437, 2935, 2853, 1603, 1497, and 1263 cm^{-1}; anal. calc. for $C_{17}H_{18}O$: C, 85.67; H, 6.61; O, 6.71; found: C, 85.99; H, 7.57.

4-[(*E*)-2-(4-chlorophenyl)ethenyl]phenol (7): white solid, 16% yield, m.p. 184–185 °C. ^{1}H NMR (CD_3OD) δ 6.83 (d, $J = 9.0$ Hz, 2H), 6.95 (q, $J = 20.7$ Hz, 2H), 7.28 (d, $J = 9.0$ Hz, 2H), 7.38 (d, $J = 9.0$ Hz, 2H), 7.40 (d, $J = 9.0$ Hz, 2H); ^{13}C NMR (CD_3OD) δ 115.33 (CH_{Ar}), 124.08 (CH=CH), 127.33 (CH_{Ar}), 127.81 (CH_{Ar}), 128.50 (CH_{Ar}), 129.29 (CH=CH), 130.22 (C_{Ar}), 132.17 ($C_{Ar}Cl$), 136.97 (C_{Ar}), 157.49 ($C_{Ar}OH$); IR (neat) 3267, 2728, 1606, 1513, 1245 cm^{-1}; anal. calc. for $C_{14}H_{11}ClO$: C, 72.89; H, 4.81; Cl, 15.37; O, 6.94; found: C, 72.66; H, 4.80.

4-[(*E*)-2-(4-hydroxymethylphenyl)ethenyl]phenol (8): the crude product was directly crystallized from MeOH/water obtaining a brown amorphous solid, 38% yield, m.p. 170–175 °C. ^{1}H NMR (CD_3OD) δ 3.85 (2H, s), 6.11 (d, $J = 8.1$ Hz, 2H), 6.35 (q, $J = 19.5$ Hz, 2H), 6.65 (d, $J = 7.5$ Hz, 2H), 6.73 (d, $J = 8.1$ Hz, 2H), 6.81 (d, $J = 7.5$ Hz, 2H); ^{13}C NMR (CD_3OD) δ 64.33 (CH_2), 113.09 ($CH_{Ar}C$), 126.22 (CH_{Ar}), 126.88 (CH=CH), 126.95 (CH_{Ar}), 127.72 (CH=CH), 128.77 (CH_{Ar}), 129.45 (CH_{Ar}), 140.46 (CH_{Ar}), 142.75(CH_{Ar}), 157.38 (CH_{Ar}); IR (neat) 3436, 2932, 2850, 1603, 1497.3, and 1263 cm^{-1}; anal. calc. for $C_{15}H_{14}O$: C, 85.68; H, 6.71; found: C, 85.69; H, 6.69.

4-[(*E*)-2-(pyridin-4-yl)ethenyl]phenol (10): yellow powder, 14% yield, m.p. 267–268 °C. ^{1}H NMR (CD_3OD) δ 6.79 (d, $J = 8.4$ Hz, 2H), 6.96 (d, $J = 16.5$ Hz, 1H), 7.41 (d, $J = 16.8$ Hz, 1H), 7.46 (d, $J = 8.4$ Hz, 2H), 7.51 (d, $J = 4.5$ Hz, 2H), 8.41 (d, $J = 4.5$ Hz, 2H); ^{13}C NMR (CD_3OD) δ 116.34 (CH_{Ar}), 121.16 (CH_{Ar}), 123.12 (CH=CH), 127.86 (C_{Ar}), 129.35 (CH_{Ar}), 133.72 (CH=CH), 145.48 (C_{Ar}), 150.58 (CH_{Ar}), 158.89 (C_{Ar}); IR (neat) 3532, 2990, 1586,

1464, and 1256 cm^{-1}; anal. calc. for $C_{13}H_{11}NO$: C, 79.16; H, 5.62; N, 7.10; O, 8.11; found: C, 78.88; H, 5.62; N, 7.10.

4-[(*E*)-2-thien-3-ylvinyl]phenol (11): white solid, 15% yield, m.p. 199–200 °C. ^{1}H NMR ($CDCl_3$) δ 6.8 (d, J = 9.0 Hz, 2H), 6.93 (q, J = 15.3 Hz, 2H), 7.20–7.21 (m, 1H), 7.31 (2H, t), 7.36 (d, J = 8.4 Hz, 2H); ^{13}C NMR ($CDCl_3$) δ 115.82 (CH_{Ar}), 121.23 (CH=CH), 121.84 (CH_{Th}), 125.06 (CH_{Th}), 126.33 (CH=CH), 127.89 (CH_{Ar}), 128.33 (CH_{Th}), 130.23 (C_{Ar}), 140.6 (C_{Th}), 158.82 (C_{Ar}); IR (KBr) 3430, 3092, 1601, 1504, and 1249 cm^{-1}; anal. calc. for $C_{12}H_{10}OS$: C, 71.25; H, 4.98; O, 7.91; S, 15.85; found: C, 71.45; H, 4.98.

4-[(*E*)-2-(2-naphthyl)vinyl]phenol (12): green solid, 15% yield, m.p. 212–213 °C. ^{1}H NMR (acetone-*d6*) δ 6.87 (d, J = 8.7 Hz, 2H), 7.28 (q, J = 15.3 Hz, 2H), 7.41–7.52 (m, 2H), 7.52 (d, J = 8.7 Hz, 2H), 7.85 (d, J = 6.0 Hz, 4H), 7.92 (s, 1H), 8.53 (s, OH); ^{13}C NMR (acetone-*d6*) δ 115.82 ($CH_{Ar}COH$), 123.65 ($CH_{Ar}CCH$), 125.80 (CH_{Ar}), 125.83 (CH_{Ar}), 126.05 ($CH_{Ar}CCH$), 126.50 (CH_{Ar}), 127.83 (CH=CH), 128.02 (CH=CH), 128.19 ($CH_{Ar}CCH$), 128.39 ($CH_{Ar}C$), 129.24 ($CH_{Ar}C$), 129.34 ($C_{Ar}CH$), 133.12 (C_{Ar}), 134.19 ($C_{Ar}CH$), 135.82 (C_{Ar}), 157.69 (C_{Ar}); IR (neat) 3395, 3051, 1597, 1510, and 1250 cm^{-1}; anal. calc. for $C_{18}H_{14}O$: C, 87.77; H, 5.73; O, 6.50; found: C, 88.99; H, 5.71.

Preparation of of 4-[(*E*)-2-(4-aminophenyl)ethenyl]phenol (9)

***t*-Butyl(dimethyl){4-[(*E*)-2-(4-nitrophenyl)ethenyl]phenoxy}silane (13)**: a solution of *t*-butyldimethylsilyl chloride (TBSCl, 1.20 mmol) in dry CH_2Cl_2 (6.0 mL) was added dropwise at 0 °C into a solution of **3** (4.14 mmol) and triethylamine (NEt_3, 0.012 mmol) in dry CH_2Cl_2 (14 mL). The reaction mixture was stirred at r.t. for 22 h and then quenched with water (4 mL). The organic layer was washed with brine (30 mL × 3), dried over $MgSO_4$, filtered, and concentrated in vacuo. The final red waxy solid (76% yield) was used without further purification. ^{1}H NMR ($CDCl_3$) δ 0.07 (s, 6H), 0.83 (s, 9H), 6.69 (d, J = 8.4 Hz, 2H), 6.84 (d, J = 16.2 Hz, 1H), 7.05 (d, J = 16.2 Hz, 1H), 7.27 (d, J = 8.4 Hz, 2H), 7.42 (d, J = 8.7 Hz, 2H), 8.03 (d, J = 8.4 Hz, 2H); ^{13}C NMR ($CDCl_3$) δ 2.78 (CH_3), 18.23 (C), 26.22 (CH_3), 114.39 (CH_{Ar}), 115.88 (CH_{Ar}), 127.45 (CH_{Ar}), 127.54 (CH_{Ar}), 129.42 (C=C), 134.0 (C_{Ar}), 137.5 (C_{Ar}), 148.8 ($C_{Ar}NO_2$), 161.1 ($C_{Ar}O$); anal. calc. for $C_{20}H_{25}NO_3Si$: C, 67.57; H, 7.09; N, 3.94; O, 13.50; Si, 7.90; found: C, 67.58; H, 7.07; N, 3.92.

4-[(*E*)-2-(4-{[*t*-butyl(dimethyl)silyl]oxy}phenyl)ethenyl]phenylamine (14): Fe powder (1.83 mmol) in 5% acetic acid (6.8 mL) was stirred at 95 °C for 30 min and cooled to 50 °C for 3 h. The solution of **14** (0.36 mmol) in EtOAc (2.5 mL) was added into the reaction mixture. The mixture was stirred at 95 °C for an additional 1 h. After being cooled to r.t., the mixture was filtered through Celite and the filtrate was washed with saturated $NaHCO_3$ (20 mL × 4); the organic phase was dried with Na_2SO_4 and the solvent was evaporated. The product **15** (brown solid, 68% yield) was used without further purification. ^{1}H NMR (DMSO-d_6) δ 0.16 (s, 2H), 0.925 (s, 3H), 5.24 (s, 2H), 6.51 (d, J = 8.4 Hz, 2H), 6.77 J 8.1 (d, J = 8.1 Hz, 2H), 6.83 (q, J = 9.6 Hz, 2H), 7.20 (d, J = 8.4 Hz, 2H), 7.35 (d, J = 8.7 Hz, 2H); ^{13}C NMR (DMSO-d_6) δ 2.78 (CH_3), 18.23 (C), 26.22 (CH_3), 114.39 (CH_{Ar}), 115.88 (CH_{Ar}), 127.45 (CH_{Ar}), 127.54 (CH_{Ar}), 129.42 (C=C), 129.80 (C_{Ar}), 130.04 (C_{Ar}), 148.55 ($C_{Ar}NH_2$), 156.77 (C_{Ar}); anal. calc. for $C_{20}H_{27}NOSi$: C, 73.79; H, 8.36; N, 4.30; O, 4.92; Si, 8.63; found: C, 73.73; H, 8.37; N, 4.32.

4-[(*E*)-2-(4-aminophenyl)ethenyl]phenol (9): *tetra-n*-butylammonium fluoride (TBAF, 1.0 M in THF, 6.15 mL, 6.15 mmol) was added into a solution of **15** (2.46 mmol) in THF (15 mL). After being stirred for 2 h at r.t., the mixture was quenched with water (25 mL) and extracted with EtOAc (3 × 30 mL). The organic phase was washed with brine (30 mL), dried over Na_2SO_4, and the solvent was evaporated. The crude product was purified by silica chromatography by using cyclohexane/EtOAc (1:1) as eluent to give **9** as brown solid, 47% yield, m.p. 250 °C dec. ^{1}H NMR ($CDCl_3$) δ 6.64 (d, J = 8.4 Hz, 2H, 6.82 (d, J = 8.7 Hz, 2H), 6.85 (2H, s), 7.28 (d, J = 8.4 Hz, 2H), 7.36 (d, J = 8.7 Hz, 2H); ^{13}C NMR ($CDCl_3$) δ 114.82 (CH_{Ar}), 115.46 (CH_{Ar}), 124.92 (CH=CH), 126.78 (CH=CH), 127.42 (CH_{Ar}), 127.63 (CH_{Ar}), 128.57 (C_{Ar}), 130.87 (C_{Ar}), 146.02 (C_{Ar}), 158.40 (C_{Ar}); IR (neat) 3437, 1614, 1512, 1250 cm^{-1}; anal. calc. for $C_{14}H_{13}NO$: C, 79.59; H, 6.20; N, 6.63; O, 7.57; found: C,79.29; H, 6.21; N, 6.61.

Biology

Cell cultures, treatments, and the MTT assay

Human PC cell lines AsPC-1, Capan-2, and BxPC-3 were cultured in RPMI 1640 medium (EuroClone) supplemented with 10% fetal bovine serum (Sigma-Aldrich, St. Louis, MO, USA), at 37 °C, 5% CO_2. Stock solutions were prepared dissolving compounds in DMSO (EuroClone), which were then diluted to the final working concentrations in culture media. In this way, the solutions were completely clear and devoid of any undissolved material by microscopic inspection. The final concentration of DMSO in the experiments was 0.1% and showed no cell toxicity.

The effects of compounds **1–12**, RSV, and 4-HSLB on PC cell viability were tested by the MTT assay (Sigma-Aldrich, St. Louis, MO, USA) following the

manufacturer's instructions. Briefly, cells were seeded in 96-well plates (4×10^3 cells/well) and incubated for 72 h with vehicle, or the test compounds. For initial screening, the compounds were tested at concentrations of 0, 20, and 100 µM (five replica wells per each condition). Subsequently, the reference and the novel compounds showing the most relevant activities on cell viability were also tested at five different concentrations ranging from 0 to 100 µM (data not shown, five replica wells per each condition). At the end of the incubation time, cells were incubated with MTT solution for at least 3 h, until purple precipitate was visible. Then, the MTT solution was removed and crystalline precipitate in each well was dissolved into DMSO. Absorbance of each well at 540 nm with background subtraction at 690 nm was quantified using a Synergy H1 microplate reader (BioTek Instruments Inc., Winooski, VT, USA).

Statistical analysis and IC_{50} calculation

Comparisons of mean values were performed using the independent samples *t*-test, using the Dunnett's test for multiple comparisons where appropriate. A *p*-value of 0.05 was considered statistically significant. IC_{50} values were calculated using the GraphPad software.

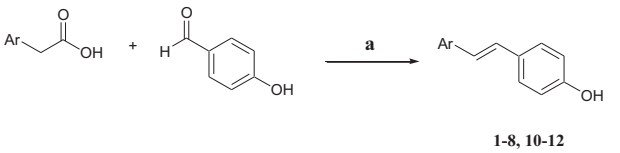

Scheme 1 Reagents and conditions. **a**: 4-hydroxybenzaldehyde (1.0 eq), arylacetic acid (1.2 eq), and piperidine (2.5 eq), 130 °C, 4–24 h, 14–38%

Antiproliferative activities of target compounds

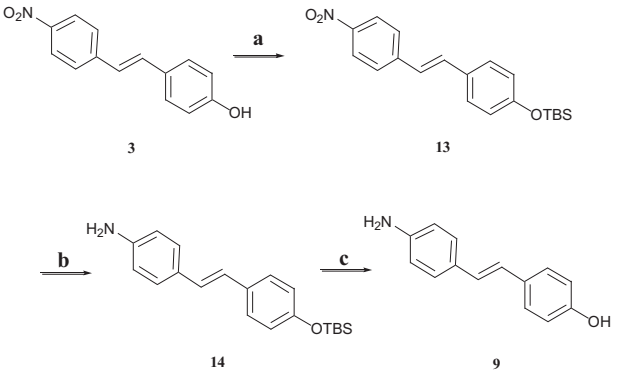

Scheme 2 Reagents and conditions. **a**: TBSCl (3 eq), Et_3N (3 eq), DCM, 0 °C - r.t. overnight, 76%; **b**: Fe powder (5 eq), 5% acetic acid, 95 °C, 68%; **c**: TBAF 1M (2 eq), THF, r.t., 3 h, 47%

Results and discussion

Chemistry

The synthesis of compounds **1–8** and **10–12** was carried out as reported in the literature (Zhang et al 2005; De Filippis et al. 2015a, 2015b; Lazer et al. 1990). The 4-hydroxybenzaldehyde and the appropriate aryl acetic acid were mixed in the presence of piperidine at 130 °C. The usual aqueous work-up and purification using silica gel column chromatography produced the desired phenols. The synthetic route is provided in Scheme 1.

The *p*-aminostilbene **9** was obtained starting from the corresponding nitro derivative **3**, treated with TBSCl in the presence of NEt_3 to form the *O*-silylated nitrostilbene **13** in CH_2Cl_2 (Kim et al. 2010). Subsequent reduction of the nitro group to the primary amine was achieved by using Fe powder in 5% acetic acid in EtOAc to give the *p*-aminostilbene *O*-protected **14**. The deprotection of **14** was carried out with TBAF in THF, giving phenol **9** (Scheme 2). Confirmation of the structure and purity of all compounds was obtained from ^1H and ^{13}C NMR and the geometry of the double bond was established by *J*-values range from 15 to 16 Hz of *trans*-olefinic proton respect of *cis*-stilbene olefinic protons from 7.4 to 8.6 Hz reported in the literature (Orgován et al. 2017).

The effects of new compounds on the viability of AsPC-1, Capan-2, and BxPC-3, three human PC cell lines with distinct genetic profiles, were evaluated by the MTT assay, one of the most sensitive and reliable indicators of cell metabolic activity, which is widely used to assess cell viability (Mosmann 1983; Florio et al. 2017, 2018; Veschi et al. 2018). It relies on the ability of dehydrogenases occurring in the mitochondria of living cells to reduce the tetrazolium dye MTT to its water-insoluble formazan salt; purple formazan crystals can be finally solubilized and quantified using a spectrophotometer. In our study, RSV and 4-HSLB were used as references. Figure 2 shows the results of the screening of the effects of novel and reference compounds on PC cell viability.

In general, all compounds affected viability of the three PC cell lines in a dose-dependent manner; in fact, the inhibition effect on viability at 100 µM is always higher than that observed at 20 µM. Specifically, at the highest concentration of 100 µM, a cell viability of <50% was observed for all tested compounds in the three cell lines, showing a good cytotoxicity, with the exception of **8** in BxPC-3 and Capan-2, and **9** and RSV in Capan-2.

The cell viability inhibition was more pronounced in AsPC-1 and BxPC-3 cell lines, where compounds **4–7** and **12** exhibited the most drastic effects, with a minimal residual cell viability. In Capan-2, only compounds **5** and **6** induced a

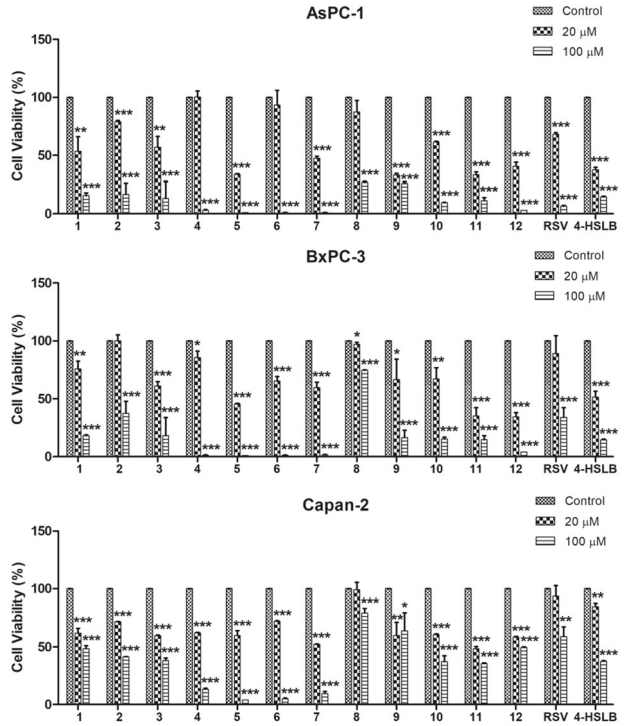

Fig. 2 Effect of compounds **1–12**, RSV, and 4-HSLB on PC cell viability. Data shown are the means ± SD of 2–3 independent MTT experiments with quintuplicate determinations. Statistically significant differences between control and each drug concentration (*$p < 0.05$; **$p < 0.01$; ***$p < 0.001$)

pronounced reduction of viability at 100 μM. At 20 μM, the results were less homogeneous, since there was a greater variability in the effects on PC cell viability, depending both by the cell line and by the tested compounds. In particular, a reduction in viability below 50% was observed only for compounds **5**, **11**, and **12** both in AsPC-1 and in BxPC-3, and for compounds **9** and 4-HSLB in AsPC-1, while other compounds had poor inhibitory activity. In Capan-2, all compounds showed a poor inhibitory effect on cell viability, which remained always above 50%, suggesting that this cell line is less sensitive to the new compounds. Regarding the reference compounds, 4-HSLB provided a better reduction of cell viability in all cases as compared to RSV, except at 100 μM for AsPC-1, suggesting that the 3,5-dihydroxy motif of RSV is not essential for the activity on PC cells. We also determined the IC_{50} values corresponding to the drug concentrations achieving a 50% inhibition of cell viability. RSV and 4-HSLB were used as reference compounds and the results are shown in Table 1.

The IC_{50} values for all tested compounds ranged from 3.03 μM to 35.34 μM. It should be noted that low IC_{50s} did not always reflect the maximum potency of cell viability inhibition. For instance, the compound showing the lowest IC_{50} (compound **9** in Capan-2 and in AsPC-1) was associated with a high residual viability in the corresponding cell lines at

Table 1 IC_{50} values for compounds **1–12**, RSV, and 4-HSLB on PC cell line viability

Compound	IC_{50}[a] (μM)		
	AsPC-1	BxPC-3	Capan-2
1	19.72 ± 0.73	21.20 ± 0.52	18.43 ± 0.93
2	21.47 ± 1.26	31.04 ± 11.87	21.10 ± 0.00
3	19.83 ± 1.26	20.01 ± 0.85	19.15 ± 0.08
4	34.52 ± 14.42	22.48 ± 0.68	20.34 ± 0.06
5	15.30 ± 0.01	19.16 ± 0.13	21.36 ± 0.52
6	30.09 ± 12.70	20.83 ± 0.25	21.22 ± 0.04
7	19.84 ± 0.09	20.49 ± 0.71	19.85 ± 0.08
8	22.95 ± 0.29	22.92 ± 1.03	21.90 ± 0.27
9	3.23 ± 0.57	22.50 ± 6.46	3.03 ± 0.49
10	20.39 ± 0.04	20.64 ± 0.71	19.29 ± 0.37
11	18.18 ± 0.33	18.38 ± 0.43	18.05 ± 0.33
12	9.46 ± 1.74	16.62 ± 1.07	11.84 ± 1.71
RSV	24.96 ± 0.83	27.98 ± 5.26	26.49 ± 7.40
4-HSLB	8.21 ± 0.29	11.73 ± 2.11	35.34 ± 0.15

[a]Data shown are the means ± SD of 2–3 independent experiments with quintuplicate determinations

100 μM, indicating that the potent effect obtained at lower concentrations was not followed by a substantially increased effect at higher concentrations, because it had already reached a plateau at low concentrations. Overall, most of the novel compounds showed IC_{50} values lower than RSV in the three PC cell lines. As regards the AsPC-1 and BxPC-3 cell lines, it is interesting to note that 4-HSLB had lower IC_{50} values than RSV, suggesting that the presence of 3,5-dihydroxy motif of RSV is not essential for cytotoxic activity in these cell lines. Moreover, 4-HSLB had lower IC_{50} values than most compounds in AsPC-1 and BxPC-3, with the exception of compound **9**, with IC_{50} of 3.23 μM in AsPC-1. Also analogs **5** and **12** had relatively low IC_{50s} in these cell lines. In Capan-2, differently from what observed in other cell lines, RSV had lower IC_{50} than 4-HSLB. Conversely, all novel *p*-substituted analogs had IC_{50} values lower than RSV and compounds **9** and **12** had the lowest IC_{50} in Capan-2 (3.03 μM and 11.84 μM, respectively). In general, the results of IC_{50} determination showed that the substitution of 3,5-dihydroxy motif of RSV with *p*-substitued phenyl (compounds **1–9**) or another aromatic ring (compounds **10–12**) played a key role in determining the inhibitory activity on PC cell lines, although it is not possible to accurately evaluate the effects of the single substituents. Another important aspect of our study on PC was the different cytotoxicity of the tested compounds against the three cell lines AsPC-1, BxPC-3, and Capan-2. Probably, this behavior was related to the inherent differences in genetic profiles, indicating cell specific effects. Compound **9**, with the polar electrondonor amino group in *p*-position, showed the lowest IC_{50} in both AsPC-1 and Capan-2 (3.23 μM and

3.03 μM, respectively), whereas its IC_{50} in BxPC-3 was higher (22.50 μM). Also the incorporation of naphthalene instead of the 3,5-dihydroxyphenyl of RSV improves the cytotoxic activity. In fact, compound **12** showed relatively low IC_{50} values, ranging from 9.46 μM to 16.62 μM in the tested cell lines. Finally, also the *p*-methyl substituted analog **5** showed relatively low IC_{50} values, ranging from 15.30 μM and 21.36 μM in the tested cell lines.

An interesting question that is currently being investigated is how known, or novel compounds exert their antiproliferative effects. For example, it has been shown that repurposed drugs may act on different targets in cancer cells and it is unclear whether these disparate targets are equally important for anticancer actions or some may be more relevant than others (Shim and Liu 2014). Therefore, also for novel molecules it is possible that antitumor activities reported could be mediated by multiple molecular targets. It is worth noting that many antitumor effects in PC have been reported also for RSV, but its mechanism of action should be further clarified. In this regard, future studies will be necessary to unravel potential biological targets mediating antitumor effects in our RSV analogs.

Conclusions

In the present study, a series of RSV analogs was synthesized and evaluated for the cytotoxic activity in three PC cell lines. Nine compounds were 4-substituted analogs of RSV without 3,5-hydroxy motif, and three compounds were obtained by introducing another aromatic ring instead of 3,5-OH phenyl. All novel compounds affected PC cell viability, with a variability that appeared structure- and cell-dependent. Several compounds (e.g., **5**, **9**, and **12**) showed an improved cytotoxic activity as compared to reference compounds, making them potential candidates for further evaluation as anticancer drugs.

Acknowledgements This study was supported by University "G. d'Annunzio" of Chieti local grants. The authors gratefully acknowledge Prof. Massimiliano Baldassarre of Institute of Medical Sciences, University of Aberdeen, for helpful comments and suggestions.

Compliance with ethical standards

Conflict of interest The authors declare that they have no conflict of interest.

References

Ammazzalorso A, De Lellis L, Florio R, Bruno I, De Filippis B, Fantacuzzi M, Giampietro L, Maccallini C, Perconti S, Verginelli F, Cama A, Amoroso R (2017) Cytotoxic effect of a family of peroxisome proliferator-activated receptor antagonists in colorectal and pancreatic cancer cell lines. Chem Biol Drug Des. 90:1029–1035

Ansari D, Tingstedt B, Andersson B, Holmquist F, Sturesson C, Williamsson C, Sasor A, Borg D, Bauden M, Andersson R (2016) Pancreatic cancer: yesterday, today and tomorrow. Future Oncol 12:1929–1946

Block G, Patterson B, Subar A (1992) Fruit, vegetables, and cancer prevention: a review of the epidemiological evidence. Nutr Cancer 18:1–29

Bonnefont-Rousselot D (2016) Resveratrol and cardiovascular diseases. Nutrients 8:250–274

Britton RG, Kovoor C, Brown K (2015) Direct molecular targets of resveratrol: identifying key interactions to unlock complex mechanisms. Ann N Y Acad Sci 1348:124–133

Carter LG, D'Orazio JA, Pearson KJ (2014) Resveratrol and cancer: focus on in vivo evidence. Endocr Relat Cancer 21:R209–R225

Chillemi R, Sciuto S, Spatafora C, Tringali C (2007) Anti-tumor properties of stilbene-based resveratrol analogues: recent results. Nat Prod Commun 2:1–15

Chou Y-C, Ho C-T, Pan M-H (2018) Stilbenes: chemistry and molecular mechanisms of anti-obesity. Curr Pharmacol Rep 4:202–209

Deck LM, Whalen LJ, Hunsaker LA, Royer RE, Vander Jagt DL (2017) Activation of anti-oxidant Nrf2 signaling by substituted trans stilbenes. Bioorg Med Chem 25:1423–1430

De Filippis B, Agamennone M, Ammazzalorso A, Bruno I, D'Angelo A, Di Matteo M, Fantacuzzi M, Giampietro L, Giancristofaro A, Maccallini C, Amoroso R (2015a) PPARα agonists based on the stilbene and its bioisosters: biological evaluation and docking studies. Med Chem Commun 6:1513–1517

De Filippis B, Ammazzalorso A, Amoroso R, Giampietro L (2019) Stilbene derivatives as new perspective in antifungal medicinal chemistry. Drug Dev Res. https://doi.org/10.1002/ddr.21525

De Filippis B, Ammazzalorso A, Fantacuzzi M, Giampietro L, Maccallini C, Amoroso R (2017) Anticancer activity of stilbene based derivatives. ChemMedChem 12:558–570

De Filippis B, Giancristofaro A, Ammazzalorso A, D'Angelo A, Fantacuzzi M, Giampietro L, Maccallini C, Petruzzelli M, Amoroso R (2011) Discovery of gemfibrozil analogues that activate PPARα and enhance the expression of gene CPT1A involved in fatty acids catabolism. Eur J Med Chem 46:5218–5224

De Filippis B, Linciano P, Ammazzalorso A, Di Giovanni C, Fantacuzzi M, Giampietro L, Laghezza A, Maccallini C, Tortorella P, Lavecchia A, Loiodice F, Amoroso R (2015b) Structural development studies of PPARs ligands based on tyrosine scaffold. Eur J Med Chem 89:817–825

De la Castra CA, Villegas I (2007) Resveratrol as an antioxidant and pro-oxidant agent: mechanisms and clinical implications. Biochem Soc Trans 35:1156–1160

de Sá Coutinho D, Pacheco MT, Frozza RL, Bernardi A (2018) Anti-inflammatory effects of resveratrol: mechanistic insights. Int J Mol Sci 19:1812–1837

Diaz-Gerevini GT, Repossi G, Dain A, Tarres MC, Das UN, Eynard AR (2016) Beneficial action of resveratrol: How and why? Nutrition 32:174–178

Ding XZ, Adrian TE (2002) Resveratrol inhibits proliferation and induces apoptosis in human pancreatic cancer cells. Pancreas 25:71–76

dos Santos JC, Bernardes A, Giampietro L, Ammazzalorso A, De Filippis B, Amoroso R, Polikarpov I (2015) Different binding and recognition modes of GL479, a dual agonist of peroxisome proliferator-activated receptor α/γ. J Struct Biol 191:332–340

Duan J, Yue W, E J, Malhotra J, Lu SE, Gu J, Xu F, Tan XL (2016) In vitro comparative studies of resveratrol and triacetylresveratrol on

cell proliferation, apoptosis, and STAT3 and NFκB signaling in pancreatic cancer cells. Sci Rep 19:31672–31682
Elshaer M, Chen Y, Wang XJ, Tang X (2018) Resveratrol: an overview of its anti-cancer mechanisms. Life Sci 207:340–349
Florio R, De Lellis L, di Giacomo V, Di Marcantonio MC, Cristiano L, Basile M, Verginelli F, Verzilli D, Ammazzalorso A, Prasad SC, Cataldi A, Sanna M, Cimini A, Mariani-Costantini R, Mincione G, Cama A (2017) Effects of PPARα inhibition in head and neck paraganglioma cells. PLoS ONE 12:e0178995
Florio R, De Lellis L, Veschi S, Verginelli F, di Giacomo V, Gallorini M, Perconti S, Sanna M, Mariani-Costantini R, Natale A, Arduini A, Amoroso R, Cataldi A, Cama A (2018) Effects of dichloroacetate as single agent or in combination with GW6471 and metformin in paraganglioma cells. Sci Rep 11(8):13610
Garcia GX, Larsen SW, Pye C, Galbreath M, Isovitsch R, Fradinger EA (2013) The functional group on (E)-4,4′-disubstituted stilbenes influences toxicity and antioxidative activity in differentiated PC-12 cells. Bioorg Med Chem Lett 23:6355–6359
Giacomini E, Rupiani S, Guidotti L, Recanatini M, Roberti M (2016) The use of stilbene scaffold in medicinal chemistry and multitarget drug design. Curr Med Chem 23:2439–2489
Giampietro L, D'Angelo A, Giancristofaro A, Ammazzalorso A, De Filippis B, Di Matteo M, Fantacuzzi M, Linciano P, Maccallini C, Amoroso R (2014) Effect of stilbene and chalcone scaffolds incorporation in clofibric acid on PPARα agonistic activity. Med Chem 10:59–65
Giampietro L, D'Angelo A, Giancristofaro A, Ammazzalorso A, De Filippis B, Fantacuzzi M, Linciano P, Maccallini C, Amoroso R (2012) Synthesis and structure-activity relationships of fibrate-based analogues inside PPARs. Bioorg Med Chem Lett 22:7662–7666
Giampietro L, Laghezza A, Cerchia C, Florio R, Recinella L, Capone F, Ammazzalorso A, Bruno I, De Filippis B, Fantacuzzi M, Ferrante C, Maccallini C, Tortorella P, Verginelli F, Brunetti L, Cama A, Amoroso R, Loiodice F, Lavecchia A (2019) Novel phenyldiazenyl fibrate analogues as PPAR α/γ/δ pan-agonists for the amelioration of metabolic syndrome. ACS Med Chem Lett 10:545–551
Herrera-R A, Castrillón W, Otero E, Ruiz E, Carda M, Agut R, Naranjo T, Moreno G, Maldonado ME (2018) Synthesis and antiproliferative activity of 3- and 7-styrylcoumarins. Med Chem Res 27:1893–1905
Huang X, Zhu HL (2011) Resveratrol and its analogues: promising antitumor agents. Anticancer Agents Med Chem 11:479–490
Jang M, Cai L, Udeani GO, Slowing KV, Thomas CF, Beecher CW, Fong HH, Farnsworth NR, Kinghorn AD, Mehta RG, Moon RC, Pezzuto JM (1997) Cancer chemopreventive activity of resveratrol, a natural product derived from grapes. Science 275:218–222
Kim JY, Lee JW, Kim YS, Lee Y, Ryu YB, Kim S, Ryu HW, Curtis-Long MJ, Lee KW, Lee WS, Park KH (2010) A novel competitive class of α-glucosidase inhibitors: (E)-1-phenyl-3-(4-styrylphenyl)urea derivatives. ChemBioChem 11:2125–2131
Kondratyuk TP, Park EJ, Marler LE, Ahn S, Yuan Y, Choi Y, Yu R, van Breemen R, Sun B, Hoshino J, Cushman M, Jermihov KC, Mesecar AD, Grubbs CJ, Pezzuto JM (2011) Resveratrol derivatives as promising chemopreventive agents with improved potency and selectivity. Mol Nutr Food Res 5:1249–1265
Kruk J, Aboul-Enein HY (2017) Reactive oxygen and nitrogen species in carcinogenesis: implications of oxidative stress on the progression and development of several cancer types. Mini Rev Med Chem 17:904–919
Lazer ES, Wong H-C, Wegner CD, Graham AG, Farinas PR (1990) Effect of structure on potency and selectivity in 2,6-disubstituted 4-(2-arylethenyl)phenol lipoxygenase inhibitors. J Med Chem 33:1892–1898
Leporini L, Giampietro L, Amoroso R, Ammazzalorso A, Fantacuzzi M, Menghini L, Maccallini C, Ferrante C, Brunetti L, Orlando G, De Filippis B (2017) In vitro protective effects of resveratrol and stilbene alkanoic derivatives on induced oxidative stress on C2C12 and MCF7 cells. J Biol Regul Homeost Agents 31:589–601
Mosmann T (1983) Rapid colorimetric assay for cellular growth and survival: application to proliferation and cytotoxicity assays. J Immunol Method 16:55–63
Murty MSR, Penthala R, Polepalli S, Jain N (2016) Synthesis and biological evaluation of novel resveratrol-oxadiazole hybrid heterocycles as potential antiproliferative agents. Med Chem Res 25:627–643
Ono K, Yoshiike Y, Takashima A, Hasegawa K, Naiki H, Yamada M (2003) Potent antiamyloidogenic and fibril-destabilizing effects of polyphenols in vitro: Implications for the prevention and therapeutics of Alzheimer's disease. J Neurochem 87:172–181
Orgován G, Gonda I, Noszál B (2017) Biorelevant physicochemical profiling of (E)- and (Z)-resveratrol determined from isomeric mixtures. J Pharm Biomed Anal 138:322–329
Queiroz AN, Gomes BA, Jr Moraes WM, Borges RS (2009) A theoretical antioxidant pharmacophore for resveratrol. Eur J Med Chem 44:1644–1649
Sadeghi A, Ebrahimi SSS, Golestani A, Meshkani R (2017) Resveratrol ameliorates palmitate-induced inflammation in skeletal muscle cells by attenuating oxidative stress and JNK/NF-κB pathway in a SIRT1-independent mechanism. J Cell Biochem 118:2654–2663
Scherzberg MC, Kiehl A, Zivkovic A, Stark H, Stein J, Fürst R, Steinhilber D, Ulrich-Rückert S (2015) Structural modification of resveratrol leads to increased anti-tumor activity, but causes profound changes in the mode of action. Toxicol Appl Pharmacol 287:67–76
Shang Y-J, Qian Y-P, Liu X-D, Dai F, Shang X-L, Jia W-Q, Liu Q, Fang J-G, Zhou B (2009) Radical-scavenging activity and mechanism of resveratrol-oriented analogues: influence of the solvent, radical, and substitution. J Org Chem 74:5025–5031
Shim JS, Liu JO (2014) Recent advances in drug repositioning for the discovery of new anticancer drugs. Int J Biol Sci 10:654–663
Stivala LA, Savio M, Carafoli F, Perucca P, Bianchi L, Maga G, Forti L, Pagnoni UM, Albinii A, Prosperi E, Vannini V (2001) Specific structural determinants are responsible for the antioxidant activity and the cell cycle effects of resveratrol. J Biol Chem 276:22586–22594
Teague A, Lim KH, Wang-Gillam A (2015) Advanced pancreatic adenocarcinoma: a review of current treatment strategies and developing therapies. Ther Adv Med Oncol 7:68–84
Telek G, Regöly-Mérei J, Kovács GC, Simon L, Nagy Z, Hamar J, Jakab F (2001) The first histological demonstration of pancreatic oxidative stress in human acute pancreatitis. Hepatogastroenterology 48:1252–1258
Tsang SW, Guan YF, Wang J, Bian ZX, Zhang HJ (2016) Inhibition of pancreatic oxidative damage by stilbene derivative dihydroresveratrol: implication for treatment of acute pancreatitis. Sci Rep 14:22859–22874
Veschi S, De Lellis L, Florio R, Lanuti P, Massucci A, Tinari N, De Tursi M, di Sebastiano P, Marchisio M, Natoli C, Cama A (2018) Effects of repurposed drug candidates nitroxoline and nelfinavir as single agents or in combination with erlotinib in pancreatic cancer cells. J Exp Clin Cancer Res 21:236
Xu Q, Zong L, Chen X, Jiang Z, Nan L, Li J, Duan W, Lei J, Zhang L, Ma J, Li X, Wang Z, Wu Z, Ma Q, Ma Z (2015) Resveratrol in the treatment of pancreatic cancer. Ann N Y Acad Sci 1348:10–19
Zhang W, Oya S, Kung M-P, Hou C, Maier DL, Kung HF (2005) Stilbenes as PET imaging agents for detecting β-amyloid plaques in the brain. J Med Chem 8:5980–5988